Membrane wetting by biomolecular condensates is facilitated by mobile tethers

Trevor GrandPre[1,2], Andrew G. T. Pyo[1], Ned. S. Wingreen[2,3,4*]

[1] Department of Physics, Princeton University, Princeton, NJ 08544, USA

[2] Center for the Physics of Biological Function, Princeton University, Princeton, NJ 08544, USA

[3] Department of Molecular Biology, Princeton University, Princeton, NJ 08544, USA

[4] Lewis-Sigler Institute for Integrative Genomics, Princeton University, Princeton, NJ 08544, USA

[*] Correspondence: wingreen@princeton.edu

Abstract

Biomolecular condensates frequently rely on membrane interactions for localization, recruitment, and chemical substrates. These interactions are often mediated by membrane-anchored tethers, a feature overlooked by traditional wetting models. Using a surface free-energy framework that couples surface tension with tether density, we solve for the contact angle and tether density in a spherical cap geometry, generalizing the Young-Dupré equation. While the contact angle retains its force-balance form, the tether density depends nontrivially on the form and strength of tether-condensate interactions. We solve for this dependence within a simple interaction model, and find a wetting phase diagram with a transition from non-wetting to partial to complete wetting over a biologically realistic parameter range. This work provides a quantitative framework for characterizing condensate-membrane interactions, uncovering potential mechanisms by which membranes mediate cellular organization and function.

Biomolecular condensates, intracellular compartments formed via phase separation, are essential for diverse biological processes, including gene regulation, metabolism, and cell signaling [1-3]. In many instances, proper condensate function relies on interactions with membranes [4-5]. These membrane interactions can spatially organize condensates, concentrate interaction partners, and facilitate access to reactants. The algal pyrenoid exemplifies this interplay: condensates enriched with the CO_2-fixing enzyme Rubisco form around traversing membranes that supply CO_2 to enhance photosynthetic efficiency. Conversely, condensates can also facilitate membrane processes such as transport, signaling, force generation, and structural remodeling. For example, Focal Adhesion Kinase (FAK) forms condensates on the cytoplasmic membrane, binding to lipids at sites where focal adhesions assemble, thereby regulating cell motility [6]. Similarly, during B cell activation, scaffold proteins in the cytoplasm form condensates that associate with the plasma membrane, a process essential for downstream signaling [3]. More broadly, unraveling the dynamic relationship between condensates and membranes is likely to be essential to understand various instances of intracellular compartmentalization.

In many cases, membrane-associated condensates do not directly wet membranes. Instead, they adhere to membrane surfaces via tethering molecules, such as proteins or specific lipids, that are anchored to the membrane. In the pyrenoid of the model alga *Chlamydomonas reinhardtii*, for example, pyrenoid-traversing membranes feature tethers like RBMP1, RBMP2, and SAGA1 which directly bind to Rubisco [7, 8]. Since membranes are typically fluid, tethers such as these are likely to be mobile within the membrane. Figure 1A illustrates a condensate

wetting a membrane through interaction with mobile tethers; because of the favorable interaction, the tethers are shown as enriched at the location of the condensate. We were motivated to ask how does tether mobility affect the condensate-membrane interaction and thus the extent of wetting?

Previous studies have explored various aspects of condensate-membrane wetting, including the effects of binding to fixed receptors on membranes [9], the influence of nonequilibrium component synthesis [10], and the role of membrane criticality on tether-mediated prewetting—characterized by a thin layer of molecules forming in domains on the membrane [11]. However, the influence of mobile tethers on condensate wetting within an otherwise uniform membrane—particularly the factors governing tether density—remains unexplored.

The wetting of a surface by a liquid is expressed by the Young-Dupré equation [12], which relates the surface tensions between the liquid, solid, and gas phases to the contact angle θ of a liquid droplet. The equation is expressed as follows:

$$\cos\theta = \frac{\sigma_{SG} - \sigma_{SL}}{\sigma_{LG}}, \qquad \text{Eq. 1}$$

where σ_{SG}, σ_{SL}, and σ_{LG} are the surface tensions of the solid-gas, solid-liquid, and liquid-gas interfaces, respectively. This equation assumes a balance of surface tensions at the contact line. For a condensate wetting a membrane, one can view the membrane as the solid, the condensate as the liquid, and the dilute phase as the gas in Eq. 1, and we will continue using this solid-liquid-gas terminology. However, mobile tethers introduce an additional dependency that is not accounted for in the classical Young-Dupré framework. Namely, the contact angle also depends

on the density of tethers, which in turn depends on the tethers' interaction strength with the condensate (see Fig. 1B).

Here, we present a generalized Young-Dupré equation that incorporates mobile tethers, bridging the gap between classical wetting theory and the unique physics of condensate wetting. Furthermore, our framework predicts the equilibrium tether density at the condensate-membrane interface as a function of the interaction strength between the tethers and the condensate. This formulation is broadly applicable and makes minimal assumptions about the specific properties of the condensate, the membrane, or the tethers.

In order to derive the equations for the contact angle and the tether density ρ_t, we start by defining the total surface free energy of a 3D condensate wetting a 2D surface as

$$F_{tot} = \sigma_{LG} \int dA_{LG} + \int \sigma_{SL}(\rho_t)\, dA_{SL} + \sigma_{SG} \int dA_{SG}\,. \qquad \text{Eq. 2}$$

Here, A_{LG}, A_{SL}, and A_{SL} are the surface areas of the liquid-gas, solid-liquid, and solid-gas interfaces, and ρ_t is the density of tethers at the solid-liquid interface. Within our framework, σ_{SL}depends on tether density, while σ_{LG} and σ_{SG} do not. The solid-liquid surface tension has this simple form (see *SI Appendix* for derivation):

$$\sigma_{SL}(\rho_t) = \sigma_{SL,0} + k_B T \left(\rho_t \ln \frac{\rho_t}{\rho_0} - \rho_t + \rho_0\right) + E(\rho_t)\,, \qquad \text{Eq. 3}$$

where $\sigma_{SL,0}$ is constant term representing the surface tension in the absence of tethers, the next term accounts for the entropic cost of bringing tethers together from a surrounding reservoir of

density, ρ_0, and the final term, $\mathrm{E}(\rho_\mathrm{t})$, accounts for interactions including condensate-tether and tether-tether (see *SI Appendix*). This framework is general, with the only assumption being that the tether density ρ_t is uniform at the membrane-condensate interface.

To analyze the model defined in Eqs. 2 and 3 and ultimately minimize the free energy with respect to the contact angle and tether density, we consider a spherical cap geometry for the condensate (Fig. 1B and *SI Appendix*). This geometry arises naturally from force balance at the liquid-gas interface and the uniform pressure within the droplet. The surface areas in Eq. 2 can be expressed in terms of the contact angle $\theta_{\rho_\mathrm{t}}$and the radius of the sphere R as

$$A_\mathrm{LG} = 2\pi R^2\left(\theta_{\rho_\mathrm{t}}\right)(1-\cos\theta_{\rho_\mathrm{t}})\,, \qquad \text{Eq. 4}$$

and

$$A_\mathrm{SL} = \pi R^2\left(\theta_{\rho_\mathrm{t}}\right)\sin^2\theta_{\rho_\mathrm{t}}. \qquad \text{Eq. 5}$$

Using the definitions of surface areas from Eqs. 4 and 5, and changing variables to express the solid-gas area in terms of the total solid area minus the solid-liquid area, $A_\mathrm{SG} = A_\mathrm{S} - A_\mathrm{SL}$, and keeping only the relevant terms (i.e. minus a global constant), the surface free energy from Eq. 2 becomes

$$F = \sigma_\mathrm{LG}A_\mathrm{LG} + \left(\sigma_\mathrm{SL}(\rho_\mathrm{t}) - \sigma_\mathrm{SG}\right)A_\mathrm{SL}. \qquad \text{Eq. 6}$$

Note that the surface free energy in Eq. 6 depends on the sphere radius R, which for a given volume V of the condensate depends in turn on the contact angle θ_{ρ_t}. To obtain a functional form for the radius, we write the volume of the droplet as

$$V = \frac{\pi R^3(\theta_{\rho_t})}{3}(1-\cos\theta_{\rho_t})^2(2+\cos\theta_{\rho_t}). \quad \text{Eq. 7}$$

The volume of the droplet is always conserved and is a constant. From Eq. 7, we can find $R(\theta_{\rho_t})$ to be

$$R(\theta_{\rho_t}) = \sqrt[3]{\frac{3V}{\pi(1-\cos\theta_{\rho_t})^2(2+\cos\theta_{\rho_t})}}. \quad \text{Eq. 8}$$

Combining Eqs. 4-8 , we obtain the final form of the surface free energy in terms of the contact angle and tether density:

$$F = \pi R^2(\theta_{\rho_t})\left[2\sigma_{LG}(1-\cos\theta_{\rho_t}) + (\sigma_{SL}(\rho_t) - \sigma_{SG})\sin^2\theta_{\rho_t}\right]. \quad \text{Eq. 9}$$

To solve for the contact angle and the tether density, we minimize the surface free energy in terms of ρ_t, which yields (*SI Appendix*):

$$\cos\theta_{\rho_t} = \frac{\sigma_{SG} - \sigma_{SL}(\rho_t)}{\sigma_{LG}}, \quad \text{Eq. 10}$$

and

$$\frac{dE(\rho_t)}{d\rho_t} = -k_B T \ln\frac{\rho_t}{\rho_0}. \qquad \text{Eq. 11}$$

Equation 10 is the generalized Young-Dupré equation. It has the same form as Eq. 1, since it simply expresses force balance, but contains the contribution of the tether density to the solid-liquid surface free energy $\sigma_{SL}(\rho_t)$ (Eq. 3). The nontrivial result is Eq. 11 which gives the tether density in terms of the function $E(\rho_t)$. For the spherical cap geometry, Eqs.10 and 11 are exact provided that ρ_t is uniform, and also hold in 2D (*SI Appendix*).

To illustrate these results, we consider a simple potential $E(\rho_t) = -\chi\rho_t$. From Eq. 11, we find the tether density to be

$$\rho_t = e^{\chi/k_B T}\rho_0, \qquad \text{Eq. 12}$$

so the contact angle is

$$\cos\theta_{\rho_t} = \frac{\sigma_{SG} - \sigma_{SL,0} + \rho_0\left(e^{\chi/k_B T} - 1\right)}{\sigma_{LG}}. \qquad \text{Eq. 13}$$

For $\chi > 0$ tethers are attracted to the condensate and are enriched at its location. This increased tether density decreases the solid-liquid surface tension as well as the contact angle, implying stronger wetting and a flatter interface. In contrast, $\chi < 0$ implies a repulsive interaction (e.g. due to steric hindrance, charge, hydrophobicity, etc.), and leads to a depletion of tethers at the condensate location, and the opposite effect on wetting.

Since χ governs the strength of wetting, there should be a critical value of χ above which the condensate completely wets the membrane (i.e. the droplet spreads out). Generically, the transition to complete wetting occurs when $\cos\theta_{\rho_t} = 1$, i.e. when $\sigma_{SG} - \sigma_{SL}(\rho_t) = \sigma_{LG}$. Physically, this condition means the preference for the solid to contact the liquid rather than the gas exactly balances the energy cost of expanding the liquid-gas interface. Using this condition and Eq. 3, we find the critical value of χ to be

$$\chi_c = k_B T \ln\left[1 + \frac{\sigma_{LG} + \sigma_{SL,0} - \sigma_{SG}}{k_B T \rho_0}\right]. \quad \text{Eq. 14}$$

To better understand how the wetting transition applies to biomolecular condensates, we can estimate the dependence of the contact angle θ_{ρ_t} on ρ_0 and χ for a typical condensate. The contact angle depends only on the difference $\sigma_{SL,0} - \sigma_{SG}$, σ_{LG}, and the reference tether density ρ_0. The difference $\sigma_{SL,0} - \sigma_{SG}$ can, in principle, be negative, indicating an attractive interaction between the condensate and the membrane in the absence of tethers, or positive, signifying a repulsive interaction. For modeling the pyrenoid and related condensates, we assume a positive value. First, based on the entropic penalty of bringing the flexible polymers in a droplet into contact with a surface, we estimate this difference to be approximately $\sigma_{SL,0} - \sigma_{SG} \sim 0.4$ mN/m (see *SI Appendix*). Second, for natural condensates, the "liquid-gas" surface tension (σ_{LG}) varies over a large range $10^{-4} - 10^{0}$ mN/m, but for concreteness we take a value of $\sigma_{LG} = 0.2$ mN/m [13]. For these parameters, in Fig. 2 we plot a heat map of $\cos\theta_{\rho_t}$ versus ρ_0 and χ, and find a large region where partial or complete wetting occurs. For an approximate reservoir tether density of $\rho_0 \sim 1/(100\ \text{nm}^2)$ as observed in human cells [14], our model predicts $\chi_c = 2.7\ k_B T$

as the binding energy per tether required for complete wetting. In general, increasing χ shifts the domain of wetting to smaller values of ρ_0.

In this work, we derived a generalized Young-Dupré equation that incorporates the interactions between condensates and mobile tethers anchored to membranes, extending classical wetting theory to biological contexts. Our model emphasizes the tradeoff between the favorable energy of tether-condensate interactions and the entropy cost of tether concentration. The generalized equation for the contact angle takes the usual Young-Dupré form, but including the dependence of the solid-liquid surface tension on the tether density. For a minimal model of this surface tension, we find that the tether density is the product of the surrounding tether density and an exponential of the tether-condensate interaction strength. For a typical tether density and condensate parameters, we find that complete wetting requires that each tether interact with the condensate with a modest energy of ~3 $k_{\mathrm{B}}T$.

To test our theory, experiments could measure the reservoir density ρ_0 and the tether density ρ_{t}. One prediction of the simple interaction model is that the ratio ρ_{t}/ρ_0 will remain constant at $e^{\chi/k_{\mathrm{B}}T}$ as reservoir density or droplet volume are varied. If this prediction is confirmed, these experiments would also provide a measurement of the tether-condensate interaction strength χ, which could be studied as a function of both condensate and tether properties. The simple model also predicts the functional dependence of the wetting angle on ρ_0 and ρ_{t}, which could also be tested. More generally, Eq. 14 relates the ratio ρ_{t}/ρ_0 to the membrane-tether interaction energy, allowing the latter to be inferred even in more complex cases. A potential experimental system for these tests is a supported lipid bilayer with either protein or DNA [15] fluorescently-tagged tethers with known affinity for a non-wetting condensate.

Our minimal model of tether-mediated wetting provides a foundation for exploring complex phenomena at condensate-membrane interfaces. Extensions could include the effects of membrane curvature [16], which alters tether density and induces geometry-dependent wetting, as well as nonequilibrium dynamics such as posttranslational modifications or active fluid coupling to membranes, which may drive directed condensate motion. For instance, active droplets propelled by internal activity gradients [17] or transport influenced by hydrodynamic flows [18] suggest mechanisms for regulating condensate dynamics. Investigating condensate-membrane wetting dynamics, including nucleation and the role of kinetic parameters like tether diffusivity, is a promising direction for understanding condensate morphology and function in biological and synthetic systems.

Acknowledgements:

We thank Martin Jonikas and Alejandro Martinez-Calvo for useful discussions. This work was supported by grants from the National Institutes of Health (R01GM140032) and from the National Science Foundation through the Center for the Physics of Biological Function (PHY-1734030) and through MCB-2410354.

Appendix A: Derivation of tether entropy

Consider a two-dimensional system of N noninteracting tethers in an area A. The entropy is given by

$$S = Nk_{\mathrm{B}}\ln\frac{A}{N}, \qquad \text{Eq. 15}$$

where k_B is Boltzmann's constant. Now, consider two compartment with areas $A_1$and A_2, and initial particle numbers N_1 and N_2. The entropy of this system is

$$S_i = N_1 k_B \ln\frac{A_1}{N_1} + N_2 k_B \ln\frac{A_2}{N_2}. \quad \text{Eq. 16}$$

Next, consider moving δN tethers from compartment 2 to compartment 1. The total entropy of this final state is

$$S_f = (N_1 + \delta N)k_B \ln\frac{A_1}{N_1 + \delta N} + (N_2 - \delta N)k_B \ln\frac{A_2}{N_2 - \delta N}. \quad \text{Eq. 17}$$

The change in the entropy is

$$\Delta S = S_f - S_i = \Delta S_1 + \Delta S_2, \quad \text{Eq. 18}$$

$$\Delta S_1 = (N_1 + \delta N)k_B \ln\frac{A_1}{N_1 + \delta N} - N_1 k_B \ln\frac{A_1}{N_1}, \quad \text{Eq. 19}$$

and

$$\Delta S_2 = (N_2 - \delta N)k_B \ln\frac{A_2}{N_2 - \delta N} - N_2 k_B \ln\frac{A_2}{N_2}. \quad \text{Eq. 20}$$

We can write the change in the entropy of compartment 1 as

$$\Delta S_1 = -\delta N\, k_B \ln\frac{N_1}{A_1} - (N_1 + \delta N)k_B \ln\frac{N_1 + \delta N}{N_1}. \quad \text{Eq. 21}$$

If we consider compartment 2 to be a large reservoir, we expand Eq. 20, since δN is much smaller than N_2:

$$\Delta S_2 \approx \delta N k_\mathrm{B}\left(1 + \ln\frac{N_2}{A_2}\right). \quad \text{Eq. 22}$$

Using Eqs. 16-22, we find that the entropy change is

$$\Delta S = \delta N k_\mathrm{B} - (N_1 + \delta N)k_\mathrm{B}\ln\frac{N_1 + \delta N}{N_1}. \quad \text{Eq. 23}$$

Now, we consider the case where the two systems are at the same density initially

$$\rho_0 = \frac{N_1}{A_1} = \frac{N_2}{A_2}. \quad \text{Eq. 24}$$

By defining

$$N_1' = N_1 + \delta N, \quad \text{Eq. 25}$$

and

$$\rho_\mathrm{t} = \frac{N_1'}{A_1}, \quad \text{Eq. 26}$$

after moving δN tethers with the entropy change in Eq. 22-23, we obtain the free-energy density in the second term on the right-hand side of Eq. 3.

Appendix B: Tether-condensate interaction energy

The solutions in Eqs. 10-11 are valid as long as the tether density in each compartment is uniform. To go farther, we consider a simple energy function corresponding to each tether interacting independently with the condensate

$$E(\rho_t) = -\chi\rho_t . \quad \text{Eq. 27}$$

However, the theory would also apply to more complex functions such as a power law expansion in ρ_t. For example, an energy function of the form

$$E(\rho_t) = -\chi\rho_t + \beta\rho_t^2 \quad \text{Eq. 28}$$

would account for tether-condensate interactions via the first term, while the second term describes tether-tether interactions, repulsive for $\beta > 0$ and attractive for $\beta < 0$.

Appendix C: Spherical cap geometry and free energy minimization

The volume of a spherical cap is

$$V = \frac{1}{3}\pi h^2\left(3R\left(\theta_{\rho_t}\right) - h\right), \quad \text{Eq. 29}$$

where $R\left(\theta_{\rho_t}\right)$ is the sphere radius as a function of the contact angle, θ_{ρ_t}, and h is the height of the spherical cap. The height of the spherical cap can be written in terms of the contact angle as

$$h = R\left(\theta_{\rho_t}\right)\left(1 - \cos\theta_{\rho_t}\right). \quad \text{Eq. 30}$$

Substituting this formula for h into Eq. 27, V gives the volume in terms of the radius of curvature and the contact angle as given in Eq. 7, and provides the equation for the radius in Eq. 8.

Now, we want to write the surface areas A_{LG} and A_{SL} in terms of the contact angle. The surface area of the spherical cap excluding the surface in contact with the solid is given by

$$A_{\mathrm{LG}} = 2\pi hR\left(\theta_{\rho_{\mathrm{t}}}\right). \qquad \text{Eq. 31}$$

Using our formula for the height gives an equation for the area in terms of the contact angle to be

$$A_{\mathrm{LG}} = 2\pi R^2\left(\theta_{\rho_{\mathrm{t}}}\right)\left(1 - \cos\theta_{\rho_{\mathrm{t}}}\right). \qquad \text{Eq. 32}$$

Lastly, let us find the area of the surface in contact with the solid. That area is

$$A_{\mathrm{SL}} = \pi a^2 = \pi R^2\left(\theta_{\rho_{\mathrm{t}}}\right)\sin^2\theta_{\rho_{\mathrm{t}}}, \qquad \text{Eq. 33}$$

where $a = R\theta_{\rho_{\mathrm{t}}}\sin\theta_{\rho_{\mathrm{t}}}$ is the radius of the circle in contact with the solid. Using Eqs. 31-33, we can minimize the surface free energy in terms of the tether density which gives the solutions in Eqs. 10-11.

Appendix D: Two-dimensional solution

The two-dimensional analogue of the surface free energy given in Eq. 2 is

$$F = \sigma_{\mathrm{LG}} l_{\mathrm{LG}} + \left(\sigma_{\mathrm{SL}}(\rho_{\mathrm{t}}) - \sigma_{\mathrm{SG}}\right) l_{\mathrm{SL}}, \qquad \text{Eq. 34}$$

where l_{LG} and l_{SL} are the lengths of the liquid/gas and solid/liquid interfaces. In two dimensions, the liquid/gas interface is the arc length of a circular cap:

$$l_{\mathrm{LG}} = 2\,R\left(\theta_{\rho_{\mathrm{t}}}\right)\theta_{\rho_{\mathrm{t}}}, \qquad \text{Eq. 35}$$

where $\theta_{\rho_{\mathrm{t}}}$is the contact angle and $R\left(\theta_{\rho_{\mathrm{t}}}\right)$ is the circle radius which is a function of the contact angle $\theta_{\rho_{\mathrm{t}}}$. The liquid/solid interface is

$$l_{\mathrm{SL}} = 2R\left(\theta_{\rho_{\mathrm{t}}}\right)\sin\theta_{\rho_{\mathrm{t}}}. \qquad \text{Eq. 36}$$

We can substitute these expressions into the surface free energy along with the definition for the liquid/solid surface tension, and we obtain

$$F = 2\sigma_{\mathrm{LG}}R\left(\theta_{\rho_{\mathrm{t}}}\right) + \left(\sigma_{\mathrm{SL}}(\rho_{\mathrm{t}}) - \sigma_{\mathrm{SG}}\right)2R\left(\theta_{\rho_{\mathrm{t}}}\right)\sin\theta_{\rho_{\mathrm{t}}}. \qquad \text{Eq. 37}$$

In order to find how the circle radius depends on the contact angle, we first compute the area of the droplet to be

$$A_{\mathrm{d}} = A_{\mathrm{arc}} - A_{\mathrm{tr}}, \qquad \text{Eq. 38}$$

where $A_{\mathrm{arc}} = \frac{1}{2}\,R^2\left(\theta_{\rho_{\mathrm{t}}}\right)$ is the area of the circular arc enclosed by the arc length that equals l_{LG}, and

$$A_{\mathrm{tr}} = \frac{1}{2}l_{\mathrm{SL}}\left[R\left(\theta_{\rho_{\mathrm{t}}}\right) - h\right] \qquad \text{Eq. 39}$$

is the area of the triangle within the circular arc area that we must subtract. From the Pythagorean Theorem, we can find the height to be

$$h = R\left(\theta_{\rho_{\mathrm{t}}}\right)\left(1 - \cos\theta_{\rho_{\mathrm{t}}}\right). \qquad \text{Eq. 40}$$

Substituting Eqs. 38-39 into Eq. 37 for A_{d}, we find that

$$A_{\mathrm{tr}} = \frac{R^2(\theta_{\rho_{\mathrm{t}}})}{2} \sin 2\theta_{\rho_{\mathrm{t}}}. \qquad \text{Eq. 41}$$

Hence, using Eq. 36-41, the area of the droplet is

$$A_{\mathrm{d}} = R^2(\theta_{\rho_{\mathrm{t}}}) \left(\theta_{\rho_{\mathrm{t}}} - \frac{\sin 2\theta_{\rho_{\mathrm{t}}}}{2}\right). \qquad \text{Eq. 42}$$

Since the area is a constant, we can solve for $R(\theta_{\rho_{\mathrm{t}}})$ in the previous equation:

$$R(\theta_{\rho_{\mathrm{t}}}) = \sqrt{\frac{A_{\mathrm{d}}}{\left(\theta_{\rho_{\mathrm{t}}} - \frac{\sin 2\theta_{\rho_{\mathrm{t}}}}{2}\right)}}. \qquad \text{Eq. 43}$$

Free energy minimization of Eq. 32, gives the same solutions as Eqs. 10-11.

Appendix E: Typical values for surface free energies

As noted in the main text, the results in Eqs. 10 and 11 depend on the difference $\sigma_{\mathrm{SL},0} - \sigma_{\mathrm{SG}}$, which quantifies the interaction between the condensate and the membrane in the absence of tethers. We study the case where this difference is positive which means that the condensate has a repulsive interaction with the bare membrane. We can roughly estimate a typical magnitude of this interaction by considering polymer condensates that tend to avoid a surface because that reduces their polymers' conformational entropy. We'd expect about 1 $k_{\mathrm{B}}T$ per polymer "blob" area in contact with the membrane, which could be ~10 nm^2, which would produce a surface energy density of $0.1 k_{\mathrm{B}}T\ /\mathrm{nm}^2$. Converting to relevant units gives $\sigma_{\mathrm{SL},0} - \sigma_{\mathrm{SG}}$~0.4 mN/m.

[1] Shin, Y., & Brangwynne, C. P. (2017). Liquid phase condensation in cell physiology and disease. *Science*, *357*(6357), eaaf4382.

[2] Banani, S. F., Lee, H. O., Hyman, A. A., & Rosen, M. K. (2017). Biomolecular condensates: organizers of cellular biochemistry. *Nature Reviews Molecular Cell Biology*, *18*(5), 285-298**.**

[3] Xiao, Q., McAtee, C. K., & Su, X. (2022). Phase separation in immune signalling. *Nature Reviews Immunology*, *22*(3), 188-199.

[4] Zhao, Y. G. & Zhang, H. Phase Separation in Membrane Biology: The Interplay between Membrane-Bound Organelles and Membraneless Condensates. *Developmental Cell* 55, 30–44 (2020).

[5] Mangiarotti, A., & Dimova, R. (2024). Biomolecular condensates in contact with membranes. *Annual Review of Biophysics*, *53*.

[6] Swaminathan, V., Fischer, R. S., & Waterman, C. M. (2016). The FAK–Arp2/3 interaction promotes leading edge advance and haptosensing by coupling nascent adhesions to lamellipodia actin. *Molecular Biology of the Cell*, *27*(7), 1085-1100.

[7] Hennacy, J. H., Atkinson, N., Kayser-Browne, A., Ergun, S. L., Franklin, E., Wang, L., ... & Jonikas, M. C. (2024). SAGA1 and MITH1 produce matrix-traversing membranes in the CO2-fixing pyrenoid. *Nature Plants*, 1-14.

[8] Meyer, M. T., Itakura, A. K., Patena, W., Wang, L., He, S., Emrich-Mills, T., ... & Jonikas, M. C. (2020). Assembly of the algal CO2-fixing organelle, the pyrenoid, is guided by a Rubisco-binding motif. *Science Advances*, *6*(46), eabd2408.

[9] Zhao, X., Bartolucci, G., Honigmann, A., Jülicher, F., & Weber, C. A. (2021). Thermodynamics of wetting, prewetting and surface phase transitions with surface binding. *New Journal of Physics*, *23*(12), 123003.

[10] Adachi, K., & Kawaguchi, K. (2021). Surface wetting by kinetic control of liquid-liquid phase separation. *Physical Review E*, *104*(4), L042801.

[11] Rouches, M., Veatch, S. L., & Machta, B. B. (2021). Surface densities prewet a near-critical membrane. *Proceedings of the National Academy of Sciences*, *118*(40), e2103401118.

[12] Thomas Young. Iii. an essay on the cohesion of fluids. *Philosophical Transactions of the Royal Society of London*, (95):65–87, 1805

[13] Wang, H., Kelley, F. M., Milovanovic, D., Schuster, B. S., & Shi, Z. (2021). Surface tension and viscosity of protein condensates quantified by micropipette aspiration. *Biophysical Reports*, *1*(1).

[14] Itzhak, D. N., Tyanova, S., Cox, J., & Borner, G. H. (2016). Global, quantitative and dynamic mapping of protein subcellular localization. *eLife*, *5*, e16950.

[15] McMullen, A., Hilgenfeldt, S., & Brujic, J. (2021). DNA self-organization controls valence in programmable colloid design. *Proceedings of the National Academy of Sciences*, *118*(46), e2112604118.

[16] Rangamani, P., Mandadapu, K. K., & Oster, G. (2014). Protein-induced membrane curvature alters local membrane tension. *Biophysical Journal*, *107*(3), 751-762.

[17] Loisy, A., Eggers, J., & Liverpool, T. B. (2019). Tractionless self-propulsion of active drops. *Physical Review Letters*, *123*(24), 248006.

[18] Shankar, S., Raju, V., & Mahadevan, L. (2022). Optimal transport and control of active drops. *Proceedings of the National Academy of Sciences*, *119*(35), e2121985119.

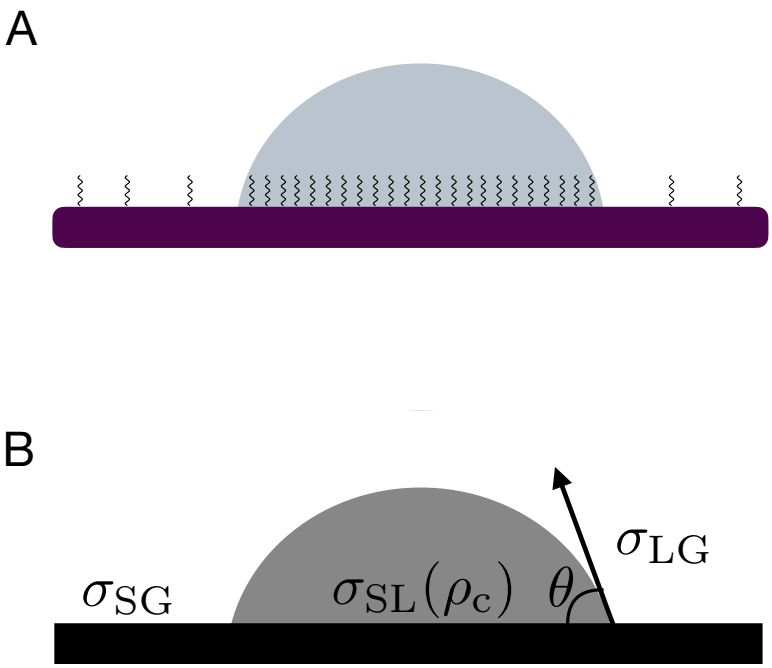

Figure 1: Wetting of a membrane by a biomolecular condensate via interaction with mobile tethers. **A** Illustration of a biomolecular condensate (blue) interacting with mobile tether molecules (black) to wet a membrane (purple). The interaction creates a localized, enrichment of tethers at the membrane-condensate interface. **B** Version of A mapped onto generalized Young-Dupré system of "solid" (membrane), "liquid" (condensate), and "gas" (dilute phase), showing the contact angle, θ, along with the surface tensions between the solid and gas (σ_{SG}), liquid and gas (σ_{LG}), and solid and liquid ($\sigma_{\mathrm{SL}}(\rho_{\mathrm{c}})$). The surface tension $\sigma_{\mathrm{SL}}(\rho_{\mathrm{c}})$) depends on the enhanced constant density of tethers, ρ_{c}, at the solid-liquid (i.e. membrane-condensate) interface.

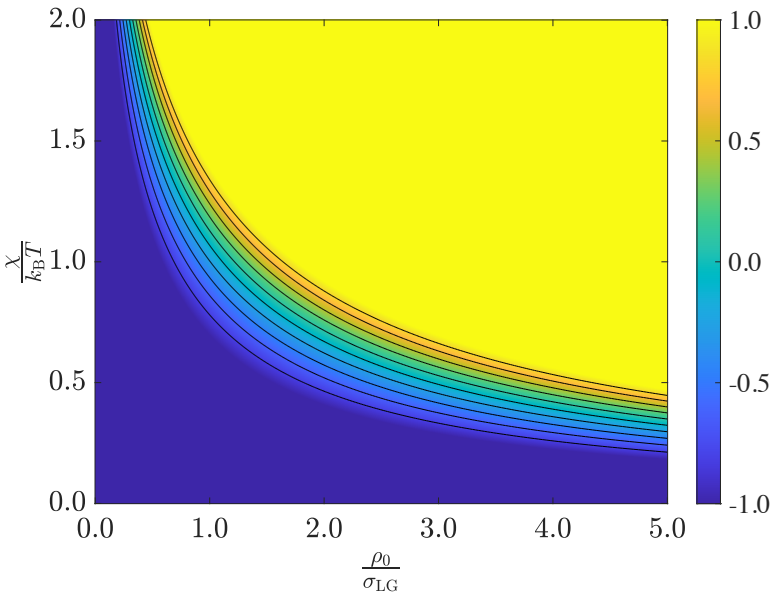

Figure 2: Phase diagram of wetting as a function of the tunable parameters χ and ρ_0. The color bar denotes the value of $\cos\theta_{\rho_t}$ from Eq. 10 with $\sigma_{SL,0} - \sigma_{SG} = 0.4$ mN/m and $\sigma_{LG} = 0.2$ mN/m. Solid black curves represent contours of constant angle between the regions of non-wetting $(\cos\theta_{\rho_t} = -1)$ and complete wetting $(\cos\theta_{\rho_t} = 1)$.